

Transport coefficients of heavy quarks around T_c at finite quark chemical potential

H. Berrehrah,¹ P.B. Gossiaux,² J. Aichelin,² W. Cassing,³ J.M. Torres-Rincon,² and E. Bratkovskaya¹

¹*Frankfurt Institute for Advanced Studies, Johann Wolfgang Goethe Universität, Ruth-Moufang-Strasse 1, 60438 Frankfurt am Main, Germany*

²*Subatech, UMR 6457, IN2P3/CNRS, Université de Nantes, École des Mines de Nantes, 4 rue Alfred Kastler, 44307 Nantes cedex 3, France*

³*Institut für Theoretische Physik, Universität Giessen, 35392 Giessen, Germany*

The interactions of heavy quarks with the partonic environment at finite temperature T and finite quark chemical potential μ_q are investigated in terms of transport coefficients within the Dynamical Quasi-Particle model (DQPM) designed to reproduce the lattice-QCD results (including the partonic equation of state) in thermodynamic equilibrium. These results are confronted with those of nuclear many-body calculations close to the critical temperature T_c . The hadronic and partonic spatial diffusion coefficients join smoothly and show a pronounced minimum around T_c , at $\mu_q = 0$ as well as at finite μ_q . Close and above T_c its absolute value matches the lQCD calculations for $\mu_q = 0$. The smooth transition of the heavy quark transport coefficients from the hadronic to the partonic medium corresponds to a cross over in line with lattice calculations, and differs substantially from perturbative QCD (pQCD) calculations which show a large discontinuity at T_c . This indicates that in the vicinity of T_c dynamically dressed massive partons and not massless pQCD partons are the effective degrees-of-freedom in the quark-gluon plasma.

PACS numbers: 24.10.Jv, 24.10.Lx, 25.75.-q, 25.75.Nq

Keywords: relativistic heavy ion collisions, transport coefficients, quark gluon plasma

The primary goal of ultra-relativistic heavy-ion experiments at the Relativistic Heavy-Ion Collider (RHIC) and the Large Hadron Collider (LHC) is to search and to characterize a new state of matter, the Quark-Gluon-Plasma (QGP), composed of partons as predicted by lattice calculations of Quantum Chromo Dynamics (lQCD). Heavy quarks are considered to be a suitable tool to study the properties of the QGP since they provide an independent scale by their heavy mass which is large compared to the temperatures that are achieved at RHIC or LHC energies in heavy-ion collisions. Initially, the heavy quarks are produced in primary hard NN collisions, which can be calculated in pQCD [1] and controlled by pp experimental data [2]. The modification of the heavy quark properties (spectral functions) in a QGP is expected to be small and their interaction is sensitive to the time evolution of the QGP essentially consisting of light quarks/antiquarks and gluons. Therefore, the difference between the initial heavy quark spectrum at production and that of final D and B mesons, observed asymptotically in the detector, is an image of the properties of the QGP during its expansion.

Different models [3–10] have been advanced to describe the heavy-quark interactions in heavy-ion collisions. The most straightforward way to compare these models is via transport coefficients which condense the complicated interactions to a few characteristic quantities. In this Letter we study the transport coefficients at finite T and finite quark chemical potential μ_q based on the DQPM model [11–13]. In the calculations presented here we limit ourselves to Born type matrix elements. The calculations

using the pole masses of the parton spectral functions and coupling constants of the DQPM model are therefore called Dressed pQCD (DpQCD) calculations. We compare our results with nuclear many-body calculations below T_c [14] and with pQCD and lQCD results at finite $T > T_c$ [6, 15].

The DQPM describes QCD properties in terms of ‘resumed’ single-particle Green’s functions (in the sense of a two-particle irreducible (2PI) approach). In other words: the degrees-of-freedom of the QGP can be interpreted as being strongly interacting massive effective quasi-particles with broad spectral functions (due to the high interaction rates). The dynamical quasiparticle entropy density s^{DQP} has been fitted to lQCD data which allows to fix for $\mu_q = 0$ the 3 parameters of the DQPM entirely (cf. Refs. [11–13] for the details of the DQPM model).

The DQPM employs a Lorentzian parametrization of the partonic spectral functions $A_i(\omega_i)$, where i is the parton species:

$$\begin{aligned} A_i(\omega_i) &= \frac{\gamma_i}{\tilde{E}_i} \left(\frac{1}{(\omega_i - \tilde{E}_i)^2 + \gamma_i^2} - \frac{1}{(\omega_i + \tilde{E}_i)^2 + \gamma_i^2} \right) \\ &\equiv \frac{4\omega_i\gamma_i}{(\omega_i^2 - \mathbf{p}_i^2 - M_i^2)^2 + 4\gamma_i^2\omega_i^2}, \end{aligned} \quad (1)$$

with $\tilde{E}_i^2(\mathbf{p}_i) = \mathbf{p}_i^2 + M_i^2 - \gamma_i^2$, and $i \in [g, q, \bar{q}, Q, \bar{Q}]$. The spectral functions $A_i(\omega_i)$ are normalized as:

$$\int_{-\infty}^{+\infty} \frac{d\omega_i}{2\pi} \omega_i A_i(\omega_i, \mathbf{p}) = \int_0^{+\infty} \frac{d\omega_i}{2\pi} 2\omega_i A_i(\omega_i, \mathbf{p}_i) = 1,$$

where M_i, γ_i are the dynamical quasi-particle mass (i.e. pole mass) and width of the spectral function for particle i , respectively. They are directly related to the real and imaginary parts of the related self-energy, e.g. $\Pi_i = M_i^2 - 2i\gamma_i\omega_i$, [11]. In the off-shell approach, ω_i is an independent variable and related to the “running mass” m_i by: $\omega_i^2 = m_i^2 + \mathbf{p}_i^2$. The mass (for gluons and quarks) is assumed to be given by the thermal mass in the asymptotic high-momentum regime. We note that this approach is consistent with respect to microcausality in field theory [16].

The DQPM model has originally been designed to reproduce the QCD equation of state, calculated on the lattice, at zero chemical potential μ_q in an effective quasi-particle approach. Since the EoS from lattice QCD is still rather unknown at finite μ_q , we use the assumption that the energy density at $T_c(\mu_q)$ is approximately independent of the chemical potential μ_q which provides $T_c(\mu_q)$ implicitly. Assuming, furthermore, that the chemical potential is identical for all flavors and employing the functional form of the parton masses from hard thermal loop calculations [17, 18, 20]:

$$M_g^2(T) = \frac{g^2(T/T_c)}{6} \left((N_c + \frac{1}{2}N_f)T^2 + \frac{N_c}{2} \sum_q \frac{\mu_q^2}{\pi^2} \right),$$

$$M_q^2(T) = \frac{N_c^2 - 1}{8N_c} g^2(T/T_c) \left(T^2 + \frac{\mu_q^2}{\pi^2} \right), \quad (2)$$

we find that a finite chemical potential μ_q can be accommodated by introducing an effective temperature

$$T^{*2} = T^2 + \frac{\mu_q^2}{\pi^2}. \quad (3)$$

The extrapolation to finite μ_q within the DQPM – assuming a constant energy density at $T_c(\mu_q)$ – leads to the approximation

$$T_c(\mu_q) = T_c(\mu_q = 0) \sqrt{1 - d^2 \mu_q^2} \quad (4)$$

with $d^2 = 8.79 \text{ GeV}^{-2}$ and $T_c(\mu_q = 0) = 158 \text{ MeV}$. Furthermore, replacing in the width $\gamma(T/T_c)$ and in the coupling constant $g(T/T_c)$ the dimensionless quantity T/T_c by $h = T^*/T_c(\mu_q)$ we have

$$\gamma_g(T, \mu) = \frac{1}{3} N_c \frac{g^2(h)}{8\pi} T \ln \left(\frac{2c}{g^2(h)} + 1 \right)$$

$$\gamma_q(T, \mu) = \frac{1}{3} \frac{N_c^2 - 1}{2N_c} \frac{g^2(h)}{8\pi} T \ln \left(\frac{2c}{g^2(h)} + 1 \right)$$

$$g^2(T^*/T_c(\mu)) = \frac{48\pi^2}{(11N_c - 2N_f) \ln \left(\lambda^2 \left(h - \frac{T_s}{T_c(\mu_q)} \right)^2 \right)} \quad (5)$$

with $\lambda = 2.42$, $c = 14.4$ and $T_s = 73 \text{ MeV}$. Eqs. (4) and (5) define the DQPM ingredients necessary for the calculations at finite temperature and quark chemical potential

μ_q . In this Letter we limit ourselves to on-shell quarks and gluons because we have found in Ref. [19] that a finite width $\gamma_{g,q,Q}$ for gluons g , light q and heavy quarks Q has an impact of about 10-20% on the heavy-quark transport coefficients.

Having the masses and the coupling constant specified we can calculate transport coefficients \mathcal{X} defined by [19]

$$\frac{d \langle \mathcal{X} \rangle}{dt} = \sum_{q,g} \frac{1}{(2\pi)^5 2E_Q} \int \frac{d^3 q}{2E_q} f(\mathbf{q}) \int \frac{d^3 q'}{2E_{q'}} \int \frac{d^3 p'_Q}{2E'_Q} \times \delta^{(4)}(P_{in} - P_{fin}) \mathcal{X} \frac{1}{g_Q g_p} |\mathcal{M}_{2,2}|^2, \quad (6)$$

where p'_Q (E'_Q) is the final momentum (energy) of the heavy quark with the initial energy E_Q . q (E_q) and q' ($E_{q'}$) are the initial and final momenta (energies) of the massless partons and $f(\mathbf{q})$ is their thermal distribution whereas $|\mathcal{M}_{2,2}|^2$ is the transition matrix-element squared for $2 \rightarrow 2$ scattering. In (6) g_Q is the degeneracy factor of the heavy quark ($g_Q = 6$) and g_p is the degeneracy factor of the massless partons ($g_p = 16$ for gluons and $g_p = 6$ for light quarks). Employing $\mathcal{X} = (E - E')$ we can calculate the energy loss, $\frac{d \langle E \rangle}{dt}(p_Q, T)$, whereas $\mathcal{X} = (\mathbf{p}_Q - \mathbf{p}'_Q)$ gives the drag coefficient, $\frac{d \langle \mathbf{p}_Q \rangle}{dt} = A(p_Q, T)$.

The spatial diffusion coefficient D_s can be expressed in two different ways [6]. It can be obtained from the slope of the drag coefficient divided by the heavy quark momentum $\eta_D = A/p_Q$,

$$D_s = \lim_{p_Q \rightarrow 0} T/(M_Q \eta_D), \quad (7)$$

as in [19]. It can also be obtained from the diffusion coefficient $\kappa = \frac{1}{3} \frac{d \langle (\mathbf{p}_Q - \mathbf{p}'_Q)^2 \rangle}{dt}$, calculated with eq. (6), as [14]

$$D_s = \lim_{p_Q \rightarrow 0} \frac{\kappa}{2M_Q^2 \eta_D^2}. \quad (8)$$

Both definitions agree if the Einstein relation is valid. In the case of the DpQCD model the deviation from the Einstein relation for small momenta p_Q is of the order 10-15%. We will adopt eq. (7) for the calculations in this Letter.

The relation (7) is strictly valid in the non-relativistic limit where bremsstrahlung is negligible, i.e. for velocities $\gamma v < 1/\sqrt{\alpha_s}$ to leading logarithm in T/m_D , where m_D is the Debye mass. Therefore, it is a good approximation for the interaction of thermal heavy quarks, $M_Q \gg T$, with a typical thermal momentum $p \sim \sqrt{MT}$ and a velocity $v \sim \sqrt{T/M} \ll 1$.

In Fig. 1 we display D_s (8) as a function of T for $\mu_q = 0$. Our results are compared with the results obtained by Moore and Teaney [6] for massless partons and $\alpha_s = 0.3$ as well as with the lattice calculations from Ref. [15]. These lattice results have recently been confirmed by the

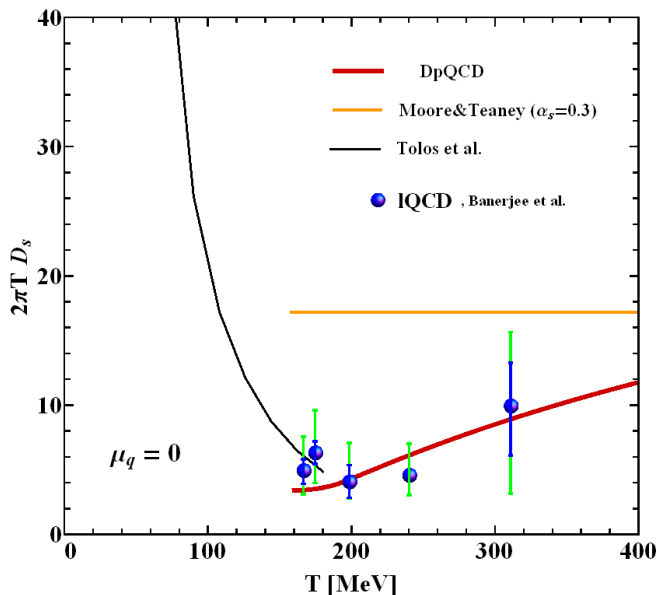


FIG. 1: (Color online) Spatial diffusion coefficient for heavy quarks, D_s , as a function of T for $\mu_q = 0$. Below $T = 180$ MeV we display the hadronic diffusion coefficient from [14], above $T = 180$ MeV that for a partonic environment. The solid orange line is the result of [6] while the red thick solid line shows the DpQCD prediction. The lattice calculations are from Ref. [15].

Bielefeld collaboration [21]. The spatial diffusion coefficient in deconfined matter is compared with the result for the spatial diffusion coefficient of a heavy meson in hadronic matter [14]. We observe that at $T = T_c$ the spatial diffusion coefficients for hadronic and partonic matter join almost continuously and agree with the lattice results. On the other hand, pQCD calculations yield a large value of the spatial diffusion coefficient as compared to the DpQCD model leading to a discontinuity of D_s close to T_c . Rapp et al. [22] have shown that the spatial diffusion coefficient in pQCD calculations can be lowered by adding nonperturbative heavy-quark interactions. Also hard thermal loop calculations with effective Debye masses and a running coupling constant lead to a substantial lowering and bring D_s to the vicinity of the lattice results [19].

These calculations can be extended to finite μ_q assuming adiabatic trajectories for the expansion. In Fig. 2 we display trajectories of constant entropy per net baryon for the hadronic as well as for the partonic phase. The latter is calculated using the effective masses of the plasma constituents in the DQPM model as well as for massless partons. For a given s/n_B the chemical potential μ_B is a monotonic function of T and therefore we can display D_s as a function of T and s/n_B . Fig. 3 displays the spatial diffusion coefficient for finite chemical potential, i.e. for different values of the entropy per net baryon s/n_B . The pQCD calculations are obtained by adding

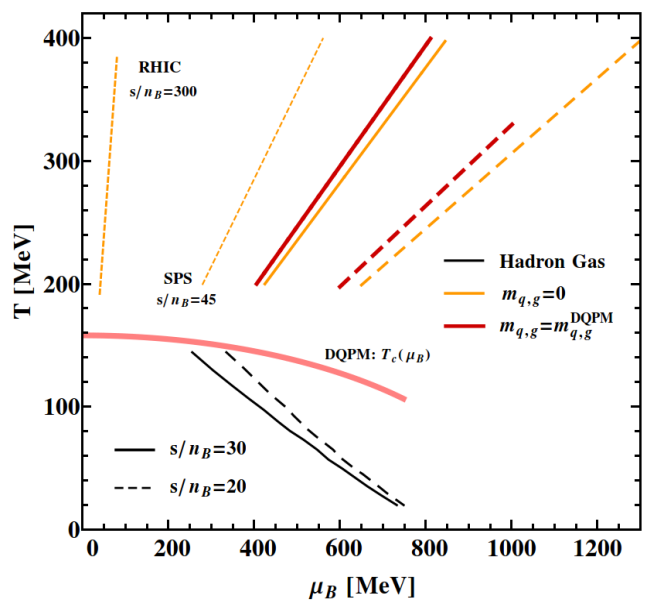


FIG. 2: (Color online) Adiabatic trajectories in the plasma and the hadron phase as a function of T and $\mu_B = 3\mu_q$. For the plasma phase we present calculations in the DpQCD model as well as for massless partons. The trajectories in the hadron phase are taken from [14]. We display as well the transition temperature $T_c(\mu_B)$ between the hadronic and plasma phase as given in the DQPM model.

the chemical potential to the thermal distributions and to the Debye mass when calculating the pQCD drag and diffusion coefficients (cf. Eq.(B13) of Ref.[6]). We observe - as in the $\mu_q = 0$ case - that the DpQCD spatial diffusion coefficient of heavy quarks approximately joins smoothly those of the hadron gas. (We expect that in the μ_B region investigated here the transition remains a cross over transition). On the contrary, pQCD calculations close to T_c are a factor of 3 higher leading to a discontinuity of the spatial diffusion coefficient, not compatible with a cross over transition as predicted by lattice calculations. This is a strong indication that close to the phase transition the effective degrees-of-freedom are massive quasi-particles and not massless quarks and gluons.

For comparing our model predictions with experimental data another transport coefficient, the energy loss of a heavy quark per unit length, $\frac{d\langle E \rangle}{dx} = \frac{d\langle E \rangle}{v dt}$, is important. It can be obtained from eq. (6) by the choice $\mathcal{X} = (E_Q - E'_Q)$. The energy loss of a heavy quark with an incoming momentum of 10 GeV/c as a function of T and μ_q in the DpQCD approach is presented in Fig. 4. As expected for a cross-over transition we observe a very smooth dependence on both variables, T and μ_q . For $\mu_q = 0$ the gluon mass depends on the temperature and therefore the increase of the energy loss is due to the change of the coupling constant. For $\mu_q = 0.2$ GeV, the energy loss is also increasing with temperature but less

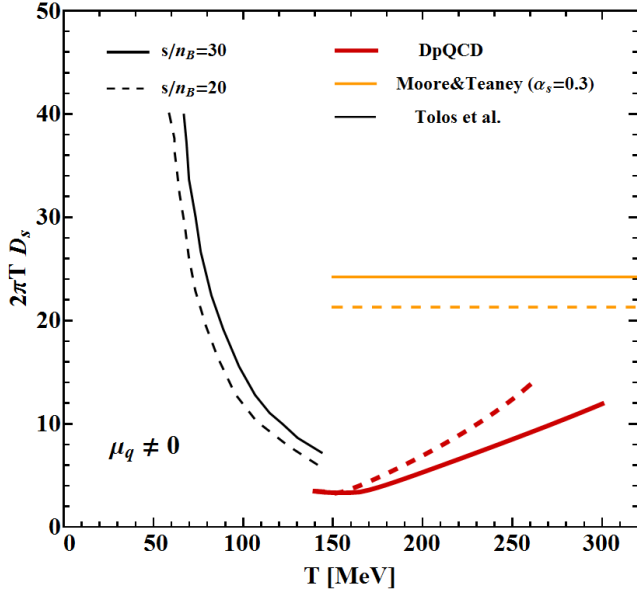


FIG. 3: (Color online) Spatial diffusion constant, D_s , as a function of T for $\mu_q \neq 0$. D_s is displayed for different values of s/n_B for a hadronic environment [14] as well as for a partonic environment. For the latter pQCD calculations are confronted with DpQCD calculations.

than for $\mu_q = 0$ because here the increase of the coupling constant is partially counterbalanced by the decrease of the effective gluon mass.

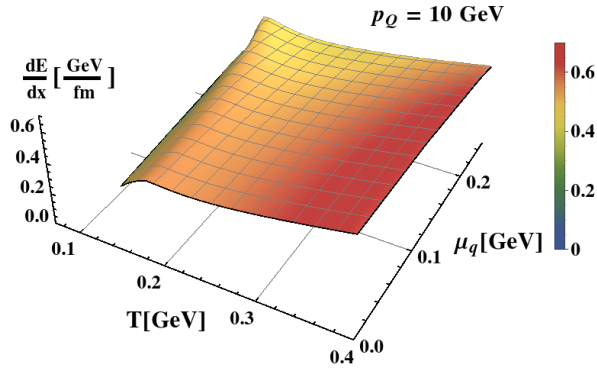


FIG. 4: (Color online) Energy loss per unit length, dE/dx , of a c -quark with incoming momentum of 10 GeV in the plasma rest frame as a function of the temperature and quark chemical potential.

We recall that the properties of the QCD medium in terms of the shear viscosity over entropy ratio η/s as well as the electric conductivity over temperature σ/T show a minimum close to T_c (cf. [23, 24]) which apparently repeats in the charm spatial diffusion coefficient reflecting a maximum in the interaction strength of the QCD

degrees-of-freedom at temperatures close to T_c .

We acknowledge the “HIC for FAIR” framework of the “LOEWE” program, the European program I3- Hadron Physics and the program “Together” of the region Pays de la Loire for support of this work and valuable discussions with V. Ozvenchuk, R. Marty and T. Steinert.

-
- [1] M. Cacciari, P. Nason and R. Vogt, Phys. Rev. Lett. , 122001**195** (2005).
 - [2] L. Adamczyk *et al.* [STAR Collaboration], Phys. Rev. D **86**, 072013 (2012).
 - [3] P. B. Gossiaux and J. Aichelin, Phys. Rev. C **78**, 014904 (2008).
 - [4] P. B. Gossiaux, J. Aichelin, T. Gousset and V. Guiho, J. Phys. G **37**, 094019 (2010).
 - [5] P. B. Gossiaux, R. Bierkandt and J. Aichelin, Phys. Rev. C **79**, 044906 (2009).
 - [6] G. D. Moore and D. Teaney, Phys. Rev. C **71**, 064904 (2005).
 - [7] H. van Hees, V. Greco and R. Rapp Phys. Rev. C **73**, 034913 (2006).
 - [8] M. Djordjevic and U. Heinz, Phys. Rev. C **77**, 024905 (2008).
 - [9] S. Cao, G. -Y. Qin and S. A. Bass, Phys. Rev. C **88**, 044907 (2013).
 - [10] H. Berrehrah, E. Bratkovskaya, W. Cassing, P.B Gossiaux, J. Aichelin, M. Bleicher, Phys. Rev. C **89**, 054901 (2014).
 - [11] W. Cassing and E. L. Bratkovskaya, Nucl. Phys. A **831**, 215 (2009).
 - [12] W. Cassing, Eur. Phys. J. ST **168**, 3 (2009).
 - [13] W. Cassing, Nucl. Phys. A **791**, 365 (2007).
 - [14] L. Tolos and J. M. Torres-Rincon, Phys. Rev. D **88**, 074019 (2013).
 - [15] D. Banerjee, S. Datta, R. Gavai and P. Majumdar, Phys. Rev. D **85**, 014510 (2012).
 - [16] L. Rauber and W. Cassing, Phys. Rev. D **89**, 065008 (2014).
 - [17] H. Vija and M. H. Thoma, Phys. Lett. B **342**, 212 (1995).
 - [18] A. Peshier, B. Kämpfer and G. Soff, Phys. Rev. C **61**, 045203 (2000). [hep-ph/9911474].
 - [19] H. Berrehrah, P. -B. Gossiaux, J. Aichelin, W. Cassing and E. Bratkovskaya, arXiv:1405.3243 [hep-ph].
 - [20] V. Ozvenchuk, O. Linnyk, M. I. Gorenstein, E. L. Bratkovskaya and W. Cassing, Phys. Rev. C **87**, 064903 (2013). [arXiv:1212.5393].
 - [21] O. Kaczmarek, Quark Matter 2014, Darmstadt, Germany, May 19-24, 2014; to be published in a special issue of Nucl. Phys. A.
 - [22] R. Rapp and H. van Hees, R. C. Hwa, X.-N. Wang (Ed.) Quark Gluon Plasma 4, World Scientific, 111 (2010).
 - [23] R. Marty, E. Bratkovskaya, W. Cassing, J. Aichelin and H. Berrehrah, Phys. Rev. C **88**, 045204 (2013).
 - [24] W. Cassing, O. Linnyk, T. Steinert and V. Ozvenchuk, Phys. Rev. Lett. **110**, 182301 (2013); T. Steinert and W. Cassing, Phys. Rev. C **89**, 035203 (2014).